Going beyond RGD: screening of a cell-adhesion peptide library in 3D cell culture

To cite this article before publication: Mariah Sarwat *et al* 2020 *Biomed. Mater.* in press https://doi.org/10.1088/1748-605X/ab9d6e

IOP Publishing Journal Title
Journal **XX** (XXXX) XXXXXX https://doi.org/XXXX/XXXX

Going beyond RGD: screening of a cell-adhesion peptide library in 3D cell culture.

Mariah Sarwat,[1] Denver Surrao,[2] Nick Huettner,[3] James A. St John,[2] Tim R. Dargaville,[1*] Aurelien Forget[4*]

[1] Institute of Health and Biomedical Innovations, Queensland University of Technology, Brisbane, Australia
[2] Clem Jones Centre for Neurobiology and Stem Cell Research, Griffith University, Gold Coast, Australia
[3] School of Chemistry, Trinity College Dublin, Dublin, Republic of Ireland
[4] Institute for Macromolecular Chemistry, University of Freiburg, Freiburg, Germany

E-mail: aurelien.forget@makro.uni-freiburg.de
E-mail: t.dargaville@qut.edu.au

Received xxxxxx
Accepted for publication xxxxxx
Published xxxxxx

Abstract

In tissue engineering, cell-adhesion peptides (CAPs) such as the ubiquitous arginine-glycine-aspartic acid (RGD) sequence have allowed the functionalization of synthetic materials to mimic macromolecules of the extracellular matrix (ECM). However, the variety of ECM macromolecules makes it challenging to reproduce all of the native tissue functions with only a limited variety of CAPs. Screening of libraries of CAPs, analogous to high-throughput drug discovery assays, can help to identify new sequences directing cell organisation. However, challenges to this approach include the automation of cell seeding in three dimensions and characterization methods. Here, we report a method for robotically generating a library of 16 CAPs to identify a microenvironment capable of directing a chain-like morphology in olfactory ensheathing cells (OECs), a cell type of particular interest for guide axon growth in spinal cord injury repair. This approach resulted in the identification of one CAPs not previously reported to interact with OECs to direct their morphology into structures suitable for potential axon guidance. The same screening approach should be applicable to any range of cell types to discover new CAPs to direct cell fate or function.

Keywords: cell-adhesion peptide, hydrogel, olfactory ensheathing cells

Introduction

In comparison to planar tissue culture polystyrene (TCPS) substrates, cell culture in 3-dimensional (3D) environments enables recapitulation of the functions of the natural extracellular matrix (ECM) missing from the 2D counterparts, including geometry and mechanical properties. While synthetic ECM hydrogels such as poly(ethylene glycol) (PEG)[1] alginate,[2] nanocellulose,[3] gelatin methacrylate[4] or carboxylated agarose[5] provide greater versatility compared to natural macromolecules such as collagen,[6] fibrin,[7] and Matrigel,[8] the synthetic hydrogels lack biological motifs to induce cell adhesion. Functionalization of synthetic hydrogels with short cell-adhesion peptides (CAPs) has led to a better understanding of the role of the ECM. CAP functionalized hydrogels have now been translated into robust 3D cell culture systems for the culture,[9] transplantation[10] and 3D bioprinting[11] of cells. However, the panel of CAPs available to design cell culture

environments has been limited to a handful of usual candidates: RGD, IKVAV, YIGSR, and PHSRN.[12]

To test the role of CAPs and precisely identify their impact on cell adhesion, high-throughput screening (HTS) approaches have been proposed.[12–15] While screening microarray platforms have been established to study cell adhesion, translating HTS to 3D cell culture systems to screen large CAP libraries presents many challenges, such as compatibility of the hydrogel with automated liquid handling systems, compatibility with biological assays, and characterization of the 3D structures. Overcoming these challenges would allow identifying the role of CAPs, not only for their cell-adhesion properties but also to identify CAP's role in driving cellular functions and organization.

Olfactory ensheathing cells (OECs) are glial cells that regenerate neural axon throughout adult life.[16] Due to their ability to guide neural axons in injured neurologic tissues, OECs have been proposed for the treatment of spinal cord injury.[17] OEC organization is crucial for guiding neural axons, but very little is known about factors regulating this process. It was suggested that the ECM composition is influencing the organisation of OECs.[18] Because OECs are support cells for neurons, OECs organisation greatly influence neuron guidance.[19] To develop spinal cord injury therapies based on OECs, it is crucial to investigate which factors regulate OEC organization in 3D.[20] It was previously reported that the ECM plays a predominant role in this process, but most of the efforts have been focusing on elucidating the role of soluble factors.[21] Therefore, in this study, we aim to use a liquid handling compatible 3D hydrogel system to screen a series of ECM-derived CAPs to investigate the role of immobilized biological cues in governing the behaviour of OECs. This study is expected to help identify a hydrogel candidate for OEC culture.[22]

The hydrogel system is based on purely synthetic 4-arm poly(ethylene glycol) terminated with vinyl sulfone groups (PEG-4VS), and thiol groups (PEG-4SH),[23] allowing the biological 'background noise' to be limited while being amendable by an automated liquid handling robot. The PEG hydrogels are functionalized with a library of CAPs comprising 16 peptides for 3D cell culture of mouse-OECs. The organisation and proliferation of the OECs triggered in response to each CAP was assessed by their morphology, immunostaining, and a metabolic assay. This study identified relevant CAPs to direct OECs organization in 3D, and these results could form the basis for developing a designer hydrogel to deliver OECs following spinal cord trauma.[24]

Results and Discussion

Mechanical properties of the cell-adhesion peptide-functionalized hydrogels.

In order for 3D cell culture hydrogels to be compatible with automatic liquid handling robots they need to have particular properties: (i) the precursors must be water-soluble, (ii) the precursor solutions need to have sufficiently low viscosity to allow for precise pipetting without creating excessive shear stresses that might damage cells, (iii) be cytocompatible and (iv) the crosslinking should occur close to ambient temperatures with kinetics slow enough to allow for the manipulation of the precursor solutions but not too slow that the cells settle and become concentrated in the bottom of the hydrogels. In addition to these requirements, hydrogel systems designed to investigate the roles of cell-adhesion peptides need to: (v) contain functional moieties compatible with rapid immobilization of CAPs.

PEG hydrogels are non-cytotoxic, the macromer precursors are water-soluble and readily available with diverse functional groups.[25] PEGs having a four-arm structures form hydrogels that can be tailored to obtain a variety of mechanical properties, including groups amendable to 'click' reactions, i.e. a rapid, irreversible, high yielding one-pot reactions compatible with water that do not generate any by-products.[26] Immobilization of peptides on polymer macromers can be achieved with diverse aqueous-based click reactions that are cytocompatible.[27] One approach is to use the thiol functional group on cysteine amino acid to couple a peptide with a polymer. Thiol functional groups can react through alkaline catalysis with vinyl sulfone groups. This reaction can occur in water at physiological pH (7.4) in a few minutes as a click reaction.[28] Therefore, we selected for the hydrogel macromers, a 4-arm PEG terminated with vinyl sulfone (**Figure 1A**) and one terminated with thiol (**Figure 1B**). This system has the advantage to use the same chemistry for the formation of the 3D hydrogel network and for the cysteine-terminated CAPs incorporation within the network. This one-pot reaction (**Figure 1C**) can be carried on at ambient temperature, physiological pH in aqueous conditions (**Figure 1D**).

To test the immobilizing of peptides into the PEG-VS/PEG-SH system, the cysteine-terminated CAP CRGDSGK was incubated with the PEG macromers and the system was allowed to react. Once the reaction was completed, a hydrogel was obtained. The hydrogel was then washed thoroughly, dried and analysed by x-ray photoelectron spectroscopy (XPS) (**Figure 1E**). PEG hydrogels terminated with either thiol or vinyl sulfone groups do not contain any nitrogen atoms, hence the presence of a peak at 396 eV in XPS, typical of N 1s binding energy, confirmed the incorporation of the CAP on the hydrogel polymer chains (**Figure 1F**).

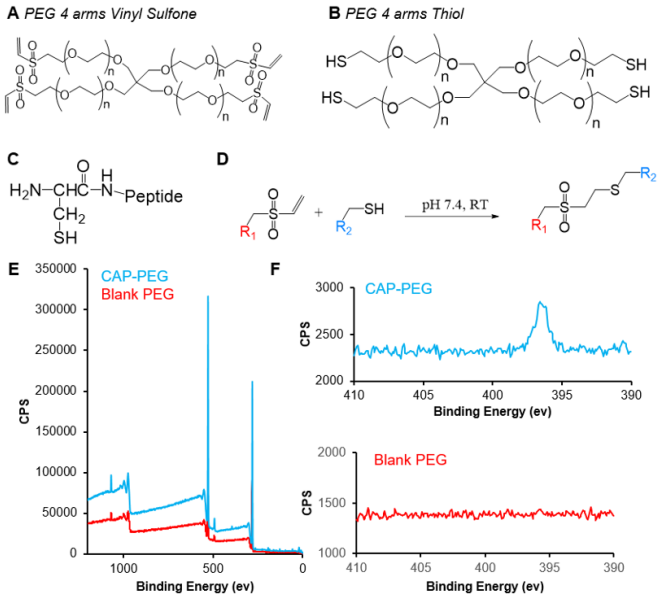

Figure 1. Chemical structure (**A**) of 4-arm poly(ethylene glycol) (PEG) terminated with vinyl sulfone functional groups PEG-4VS, (**B**) of 4-arm PEG terminated with thiol functional groups PEG-4SH, and (**C**) of cysteine terminated peptide. The chemical reaction between vinyl sulfone and thiol. X-ray photoelectron spectroscopy of PEG hydrogel (red) and peptide functionalised PEG hydrogel (blue) for (**E**) the survey scan, and (**F**) high-resolution spectra with nitrogen peak showing the functionalization of the PEG hydrogel with cell-adhesion peptide.

Automation of the 3D cell culture synthesis requires estimation of the gelation time in order to adapt the liquid handling robot protocol to the hydrogel system. The crosslinking kinetics of the PEG-4SH / PEG-4VS hydrogel system were measured by rheology. It was found that the PEG-4SH macromers react with the PEG-4VS to form stable hydrogels in 4.3 ± 1.7 min (as defined by the crossover in G' and G") (**Figure 2A and 2B**). It is well-accepted that the mechanical properties of 3D cell culture substrate play a role in the fate and function of cells.[29] Therefore, the shear modulus of the fully reacted hydrogel was assessed. On a plate-plate rheometer, the storage modulus of the PEG hydrogels was measured (G') of 7.0 ± 0.4 kPa (**Figure 2C and 2D**). Because the PEG hydrogels are crosslinked with a thiol functional group, the cysteine-terminated CAPs are competing with the formation of hydrogel crosslinking and impact the mechanical properties of the hydrogel. Because the same molar ratio of peptide to polymer was used for each hydrogel we can assume the number of vinyl sulfone groups consumed by incorporation of the peptide will be similar, and hence mechanical properties. However, this assumes similar reactivity of the different thiols in the various peptides. This is a disadvantage of the high throughput method, but one that is not easily avoided. To simulate the incorporation of peptides into the hydrogel network, hydrogels were functionalised with mercaptoethanol and the shear modulus was assessed. We observed that the incorporation of a thiol competing group retards the hydrogel gelation to 12.3 ± 0.64 min (**Figure 2A and B**) but also reduces the shear modulus of the final hydrogel to a G' of 2.1 ± 0.4 kPa (**Figure 2C and D**). However, this shear modulus is within the range reported for brain tissues between 1.4 kPa[30] and 2.4 kPa,[31] and grey matter at 4.5kPa[32] – relevant to OECs. Therefore, the ratio of CAP incorporated to the hydrogel and the hydrogel concentration was kept identical for the subsequent experiments.

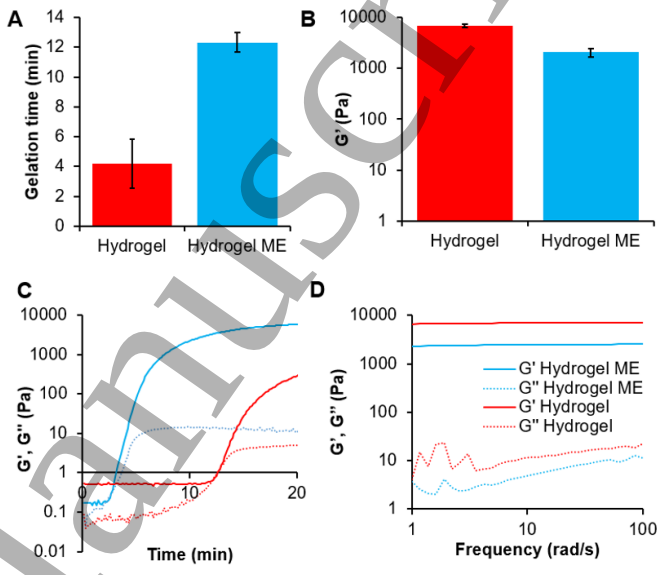

Figure 2. Poly(ethylene glycol) (PEG) hydrogels and PEG hydrogels functionalized with mercaptoethanol to simulate the incorporation of peptide: (**A**) Gelation time measured at the intersection of storage (G') and loss modulus (G") (**B**) Time sweep of G' and G" curve showing the gel point (**B**) Shear modulus G' at 60 rad/s (**D**) Frequency sweep showing G' and G" for both hydrogels. Histograms show the average for n= 3, error standard deviation.

Automated screening of a cell-adhesion peptide library in hydrogels.

Understanding the role of immobilized signals in OECs organization requires the establishment of a variety of 3D synthetic environments. In synthetic hydrogels, this means functionalizing the network with different cell-adhesion motifs. If done manually, this task can be tedious and time-consuming. Automation of both CAP functionalization and incorporation of the OECs within the hydrogel facilitate increasing the number of screened samples without reducing the reproducibility. Screening of CAPs has been proposed on microarrays where a few cells are contained on a spot of hundreds of µm. While on such arrays many assays can be performed with keeping the working volumes and quantity of

reagents to a minimum, the observation of the cell response to a library of CAPs has limited the observation of their behaviour in 2D, and do not allow to study the cell organisation in a 3D environment.[14] To investigate the impact of CAPs in directing 3D organization requires cell microenvironments with a substantial volume. Therefore, we developed a screening platform with 15 µL hydrogels in a trade-off between the amount of reagents required and the ability to observe multi-cell interactions and changes to morphology. The larger volume also means the approach can be adapted to any robotic dispensing system capable of pipetting resolution down to approximately 0.01 µL.

The viscoelastic data provided critical information on the gelation time of the PEG-4VS / PEG-4SH system (12 min). With this, we designed a program capable of manipulating the hydrogel precursor solutions, OEC suspension and peptides to form 3D cell culture environments (**Figure 3**). To prepare samples in triplicate, the PEG-4SH solution was pipetted into three wells of a 384 well-plate. Then, a master mix was prepared in a 96 well-plate comprising of the PEG-4VS solution and the CAP solution to which the cell suspension was added. This was then homogenized by successive oscillating pipetting. The homogenized solution was then added to three 384 wells and further homogenized by successive oscillating pipetting. The whole procedure had to be performed in less than 12 minutes to avoid gelation of hydrogels during handling. By adding the reagents in this order and doing the three replicates for each CAP before moving to the next one allowed the liquid handling robot to be programmed to perform the hydrogel assembly for one condition in one minute – well within the gelation window. These steps were then repeated for each hydrogel functionalized with a different CAP. In total 16 CAP hydrogels, each with a volume of 15 µL could be prepared in triplicate in less than 15 minutes. Once complete, media was added to avoid the cells being starved for an excessive amount of time.

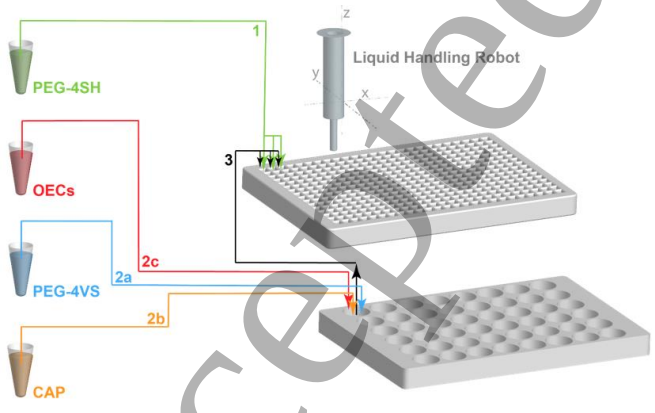

Figure 3. Schematic of the automation protocol for the preparation of 3D cell microenvironments with olfactory ensheathing cells (OECs) embedded in poly(ethylene glycol) (PEG) hydrogels constituted of two 4-arm PEG macromers terminated with either thiol functional groups (PEG-4SH) or vinyl sulfone functional group (PEG-4VS). The hydrogels are functionalized with cell-adhesion peptides CAP.

Olfactory ensheathing cells attached to cell-adhesion peptide-functionalized hydrogels

In the 3D cell culture environments, the OECs spreading was followed over 14 days to validate the automated methods. We compared the cell spreading of the OECs on tissue culture polystyrene (TCPS) with blank PEG, and PEG functionalized with CRGDSGK (**Figure 4**). After 7 days no cell spreading was observed in either the blank PEG or in the CAP-functionalized PEG. After 14 days in the biologically inert blank PEG hydrogels, the cells remain rounded,[33] and only on the TCPS and in the CAP-functionalized PEG, cell spreading was visible. Therefore, the subsequent experiments were performed with 14 days incubation.

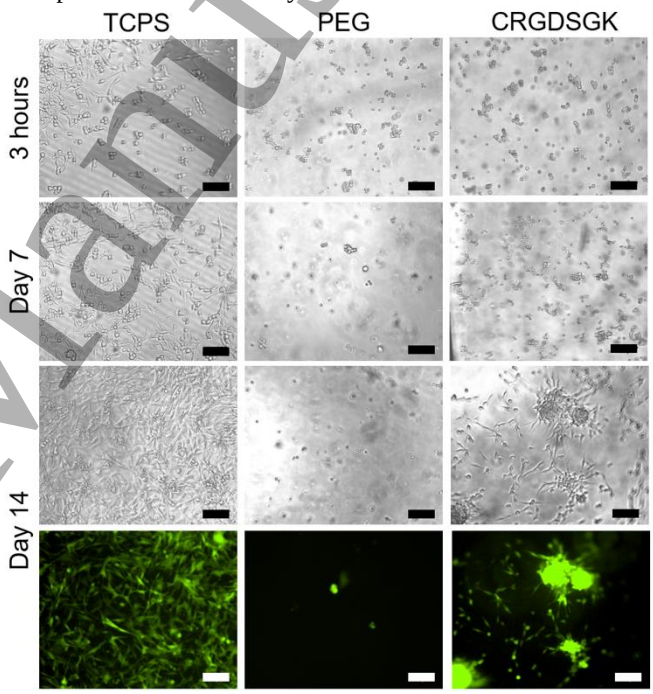

Figure 4. Microscopic images of olfactory ensheathing cells (OECs) organization on tissue culture poly(styrene) (TCPS), blank poly(ethylene glycol) (PEG) and PEG hydrogel functionalized with the peptide sequence CRGDSGK after 3 hours, 7 days and 14 days after seeding. Bright-field images and fluorescent images of the OEC tagged with a green fluorescent protein. Scale bar 100 µm, pictures representative of three technical replicates.

Discovery of cell-adhesion peptides to drive olfactory ensheathing cells organisation.

To induce cell adhesion in synthetic hydrogels such as PEG, it is required to functionalise the hydrogel with

biological cues such as CAPs. However, little information is available on the potential of CAPs to drive cell organisation and in particular OECs. We selected 16 different CAP sequences. The CAPs have been selected based on a library previously published.[12] The 16 CAPs were selected to represent diverse macromolecules of the ECM, within one macromolecule to target diverse cell receptors. Only peptides devoid of cysteine in the sequence were chosen to circumvent interference with the binding to the polymer.

Thus, the CAPs could only be immobilized on the PEG through the terminated cysteine added at the end of the cell-adhesion motif. These CAPs were selected based on our previous theoretical framework[12] to represent adhesive sequences from different ECM macromolecules and to target different receptor of the cell membrane. The cell microenvironments were prepared following the automated sequence developed explicitly for these hydrogels, and the resulting OECs organization was observed after 14 days (**Figure 5**).

On TCPS, the OECs organized into a spindle shape typical of cells cultured on a planar substrate. As previously observed in the control experiment above, the OECs maintained a rounded shape in the blank PEG hydrogels. A rounded shape was also observed in several CAPs of our library: CSVVYGLR, CGFGER, CKAEDITYVRLKF, CMNYYSNS, CVPGIG, and CIDAPS. This rounded shape might have several origins: the CAPs is not recognised by the cell receptor, the targeted cell receptor is not expressed by the cells in the 3D substrate, the CAPs concentration is too low to induce morphological change or the hydrogel stiffness is not adequate for the CAPs. In contrast, the OECs spread into a spindle shape like on TCPS in the PEG hydrogels functionalized with CRGDSGK, CIKVAV, CYIGSR, CAELDVP, CDGEA, and CTWYKIAFQRNRK. OECs have been shown to be positive for β1, α4, α6 and α7 integrins but negative for β4, α1 and α3. It is therefore unexpected to have CIKVAV binding to integrin α3β1. Conversely, for CLDV and CLALERKDHSG, the OECs organised into spheroids. Interestingly, the sequences CPRARI directed the OECs to form a chain organization and the CKRSR directed a spheroids organization. Both CPRARI and CKRSR, while not previously reported to induce OEC adhesions, bind to α4β1 integrin and heparin receptors, respectively. This demonstrates that the screening approach allows identifying positive CAPs "hits" that could not be predicted based on current knowledge.

The cellular organizations help us to identify CAP candidates that could be used to direct OECs into structures able to improve spinal cord injury recovery. Usually, OECs having a spindle shape are associated with rapid migratory behaviour,[34] whereas chain-like organisation is identified as a growth substrate for neurons.[22] Therefore, the chain-like organization could potentially be a favourable OEC organisation to improve axon extension, but this will have to be validated in animal models.

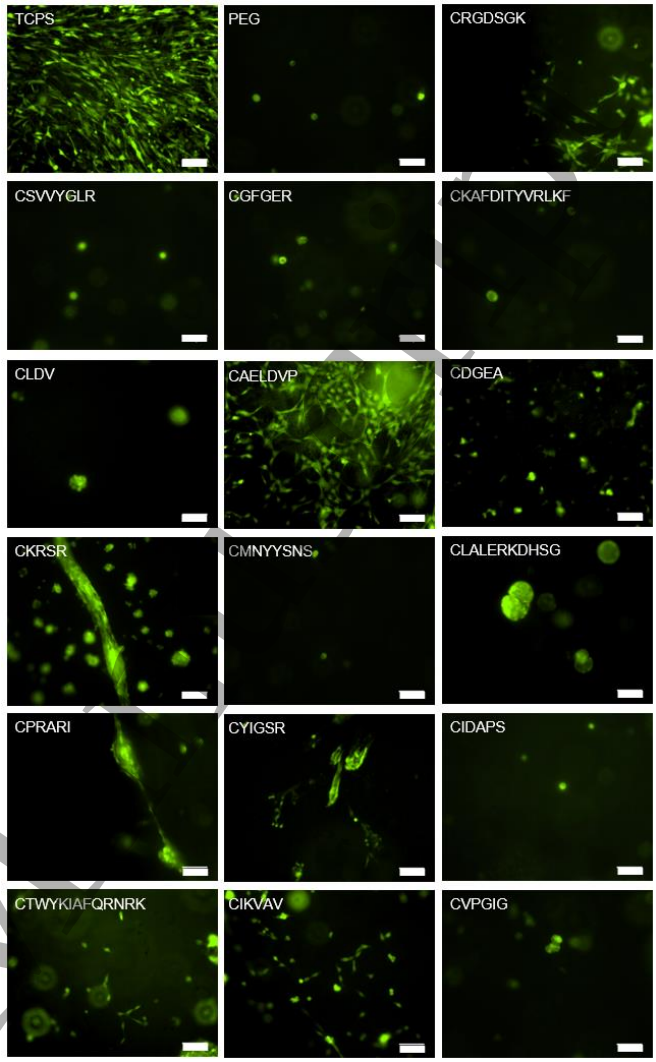

Figure 5. Microscopy images of olfactory ensheathing cells (OECs) expressing green fluorescent protein (GFP) culture on tissue culture poly(styrene) (TCPS), poly(ethylene glycol) (PEG) hydrogels and PEG functionalized with cell-adhesion peptides (CAPs). Scale bar 100 µm.

The CAP library was selected to mimic seven different ECM macromolecules (**Table 1**). However, the spinal cord is principally composed of collagen, laminin, fibronectin, and proteoglycans.[35] The CAP that trigger the chain-like organization is a sequences originating from fibronectin (CPRARI) and the spheroid organisation was triggered by a CAP from osteopontin (CKRSR) – a molecule associated with bone maturation,[36] and tumour cell proliferation.[37] These peptide sequences bind to the α4β1,[38] and heparin receptor,[39] respectively. In a quest to better understand the OEC organization triggered by the CAPs, we classified the sequences by macromolecules of origin, targeting receptor, and observed morphology (**Table 1**). However, a particular

cell organization could not be linked to a specific macromolecule or to a cell receptor.

Table 1. Tested peptide library targeting different cell surface receptors and their respective impact on olfactory ensheathing cell (OEC) morphology and organization.

Origin	*Peptide*	*Receptor*	*OEC*	*Neurons*	*Morphology*
	TCPS	-	-	-	spindle
	PEG	-	-	-	round
Fibronectin	CRGDSGK	$\alpha_v\beta_3$, $\alpha_v\beta_5$ [40]	[41]	[42]	spindle
	CIDAPS	$\alpha_4\beta_1$[43]	-	-	round
	CLDV	$\alpha_4\beta_1$[44]	-	-	spheroids
	CPRARI	$\alpha_4\beta_1$[38]	-	-	***chains***
Laminin	CIKVAV	$\alpha_3\beta_1$ [45]		[46]	spindle
	CKAFDITYVRLKF	$\alpha_6\beta_1$, $\alpha_v\beta_3$[47]	-	-	spindle
	CTWYKIAFQRNRK	$\alpha_6\beta_1$[48]	-	-	round
	CYIGSR	$\alpha_4\beta_1$[49]	-	[50]	spindle
Osteopontin	CKRSR	Heparin [39]	-	-	***chains***
	CSVVYGLR	$\alpha_4\beta_1$[51]	-	-	round
Collagen I	CGFGER	$\alpha_2\beta_1$[52]	-	-	round
	CDGEA	$\alpha_2\beta_1$[53]	-	-	round
Collagen IV	CMNYYSNS	$\alpha_v\beta_3$ [54]	-	-	round
Elastin	CVPGIG	-[55]	-	-	round
THBS1	CAELDVP	$\alpha_4\beta_1$[56]	-	-	spindle
	CLALERKDHSG	$\alpha_6\beta_1$[57]	-	-	spheroids

Hydrophobic, polar uncharged, *polar charged* and cysteine, THBS1: Thrombospondin-1

CRGDSP, CPRARI and CKRSR cell-adhesion peptides do not alter olfactory ensheathing cell phenotype.

In addition to a chain organization, OECs, to be valuable for spinal cord injury repairs, need to express the neurotrophin membrane receptor (p7NTR), a marker characteristic of this lineage. Immunostaining of the OECs cultured in the PEG hydrogels functionalized with CRGDSGK, CPRARI and CKRSR showed that p7NTR was expressed similarly to the OECs cultured on TCPS (**Figure 6**). While the peptide CRGDSGK directed the organization of OECs into a typical spindle shape, conservation of the hallmark of OEC suggests that the chain organization induced by the CPRARI and the spheroid organisation induced by CKRSR sequences do not modify the OEC lineage, suggesting the potential use of these CAPs for designing cell delivery hydrogels. This result further implies that screening library of CAP allows identifying relevant peptide sequences to direct the organization of cells into structures pertinent for tissue regeneration.

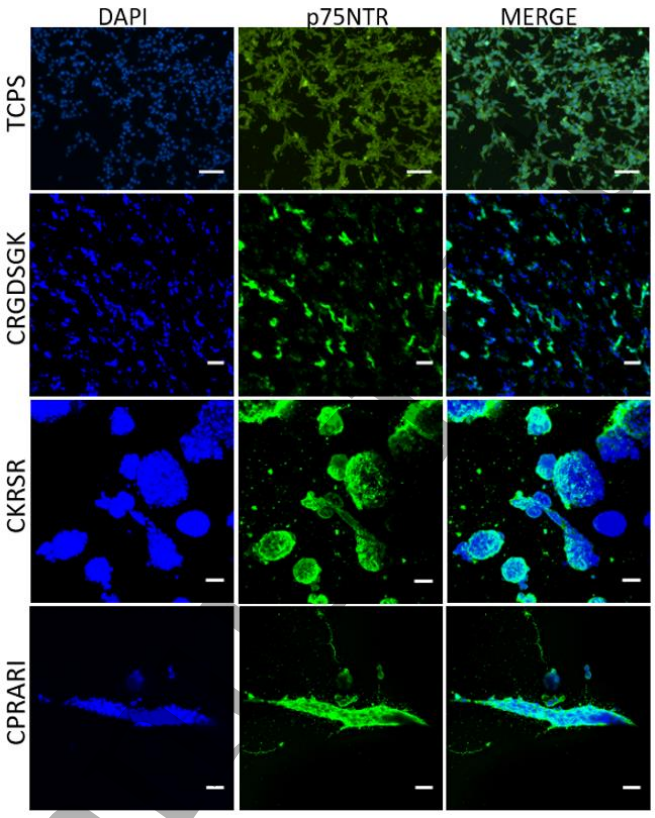

Figure 6. Immunostaining of olfactory ensheathing cells (OECs) after 14 days of culture on 2D tissue culture polystyrene (TCPS) substrate compared to cells cultured in poly(ethylene glycol) hydrogels functionalised with CRGDSGK, CKRSR or CPRARI cell adhesion peptides. Cells are labelled in blue for the nuclei and green for the p7NTR protein, showing OEC phenotype is preserved in the CAP functionalized hydrogels. Confocal images. Scale bar is 100 µm.

The organisation of the OECs in the 3D cell culture substrate was further characterised by reconstructing the cell volume (**Figure 7**). The 3D image allows for the visualisation of the 3D morphology presented by the cells in the hydrogel.

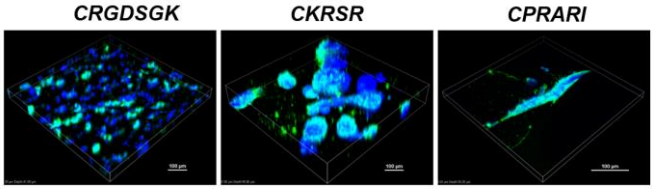

Figure 7. 3D reconstructed confocal images showing the shape of the cells in the 3D cell culture substrate. Blue: DAPI, Green: p75NTR.

CPRARI, CKRSR, and CRGDSGK cell-adhesion peptides drive olfactory ensheathing cell proliferation.

Cell transplantation for tissue repair requires the injection of the cells encapsulated in a hydrogel that preserves cell phenotype and induced cell proliferation to create new tissue. The selected CAPs: CRGDSGK, CPRARI, and CKRSR preserve OECs phenotypes. Metabolic activity of OECs in these three CAP-functionalised hydrogels was compared to TCPS by measuring the metabolic activity of the cells on day 7 and day 14. As previously observed, OECs at day 7 are not yet organised in any particular shape in the CAPs modified hydrogels. In fact, OECs morphology at day 7 is similar in all observed conditions. Only at day 14, OECs show rounded shape in blank PEG hydrogel, in CRGDSGK-functionalized hydrogels OECs exhibit a typical elongation for cells cultured in RGD hydrogels, a spheroid organisation in CKRSR-functionalized hydrogels and a chain-like shape in CPRARI-functionalized hydrogels (**Figure 8A**).

In all three CAPs, an increase of metabolic activity was measured between the two-time points. Cells cultured in the PEG hydrogels functionalized with CRGDSGK showed a 3.1-fold increase in cell metabolic activity. In CPRARI a 2.8-fold increase and in CKRSR a 2.9-fold increase were observed. This result suggests that the CAPs support the cell growth to a greater extent than TCPS substrates where a 1.7-fold increase was observed (**Figure 8B**). While the metabolic activity in CKRSR and CPRARI was slightly lower than in CRGDSGK functionalized hydrogels. The difference of cell viability at day 7 between TCPS and 3D CAP-functionalized hydrogel might come from the difference in volume, where cells in 3D have more space to grow than on 2D. At day 14, the cells on TCPS might be close to being confluent and the cell proliferation come to a stall. The TCPS at day 7 was used to be able to normalize the cell growth across different condition and time points. As suggested by the higher cell proliferation in CAPs-functionalised hydrogel compare to the non-functionalised PEG, the CAPs might also stimulate the proliferation. In addition, similar cell viability is observed in CRGDSGK, CKRSR and CPRARI indicating that the organization of the cells into chain-like or spheroid structure does not affect the cell metabolic activity. This is a critical property in designing hydrogels to be used as cell carriers for spinal cord injury because such hydrogels could allow supporting cell growth after injection.

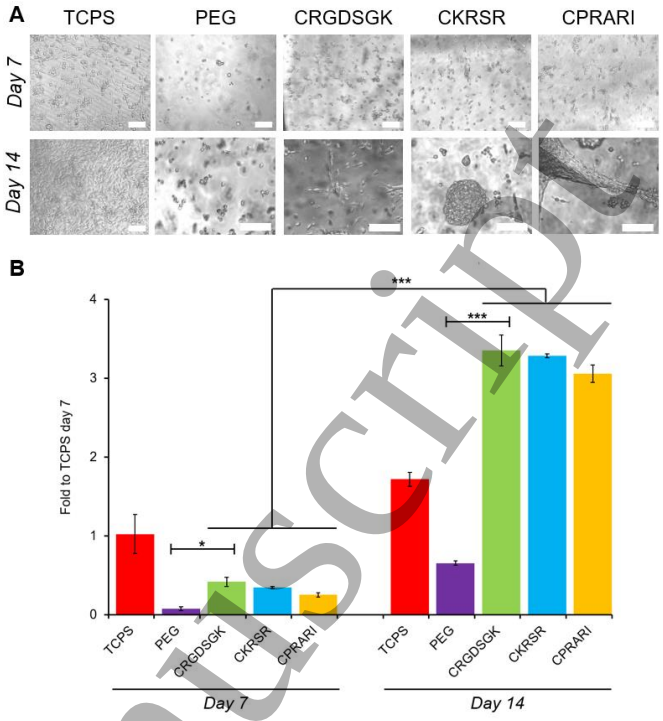

Figure 8. Olfactory ensheathing cells (OECs) at day 7 and day 14 on 2D tissue culture polystyrene (TCPS) compared to blank poly(ethylene glycol) hydrogel (PEG) and PEG hydrogels functionalized with CRGDSGK or CKRSR or CPRARI cell adhesion peptides. (**A**) Brightfield microscopic picture, scale bar 100 µm. (**B**) Histogram show average of the cell viability measurement for n= 3, error bars show standard deviation and t-test two-tail statistical analysis with * $p<0.05$, ** $p<0.01$ and *** $p<0.001$.

Materials and Methods

Materials

Thiol functionalised poly(ethylene glycol) 4-arm (PEG-4SH) with a MW = 5000 g.mol-1 and 4-arm poly(ethylene glycol) vinyl sulfone (PEG-4VS) with a MW = 20,000 g.mol-1 were purchased from Jenkem Technology, USA. All cell-adhesion peptides (CAPs) sequences: CGFGER, CDGEA, CKIVAV (laminin E1-4, E1 and E8), CYIGSR (laminin B1), CTWYKIAFQRNRK (laminin γ1), CKAFDITYVRLKF (laminin γ1), CIDAPS, CLDV, CPRARI, CKRSR, CSVVYGLR, CVPGIG, CRGDSGK, CMNYYSNS, CAELDVP and CLALERKDHSG were purchased as 95% pure by HPLC from GenScript Biotech, China. Genetically modified Green Fluorescent Protein (GFP) positive Olfactory Ensheathing Cells (OECs) were a gift from Filip Lim, Universidad Autonoma de Madrid, Spain and characterised as previously described.[58] Dulbecco's modified Eagle medium (DMEM/F12), Dulbecco's Phosphate Buffer Saline (dPBS), Penicillin-streptomycin solution (10,000 U/ml) and TrypLE Express Enzyme (cell-dissociation enzyme) were purchased

from ThermoFisher Scientific, Australia and fetal bovine serum (FBS) from Corning, Australia. Well-plates in a 384-flat glass-bottom format were purchased from Cellvis LLC, USA. 200 µl strip tubes from Sarstedt, Australia and 1.5 ml tapered tubes from Thomas scientific, Australia. 50 µl robotic filter tips were purchased from Qiagen, Germany. Primary antibodies p75NTR (1:100, Cat#839701, BioLegend, USA), Alexa FluorTM 488, and DAPI (1:500, Cat# D1306) were obtained from ThermoFisher Scientific, USA. 4% paraformaldehyde solution was purchased from ThermoFisher Scientific, Australia. Bovine Serum Albumin (BSA) and Triton™ X-100 purchased from Sigma Aldrich, Australia. And (WST-1) Cell Proliferation Assay Kit was obtained from Roche Applied Science, Germany.

Methods

Preparation of Peptide Functionalised hydrogels

Peptides with less than six amino acids were dissolved in phosphate-buffered saline (PBS pH = 7.4) at a concentration of 138.5 mM. Longer peptides sequences and hydrophobic sequences were first dissolved in DMSO and then diluted in PBS pH = 7.4 to a final concentration of 138.5 mM. Hydrogels were prepared by thiol-Michael addition between PEG-4VS and PEG-4SH in a molar ratio of 1.5:1. The reaction was carried at room temperature, pH 7.4. Peptides were incorporated in the polymer network by Michael-type addition between the vinyl sulfone terminated PEG and the thiol of the cysteine terminated peptides. Stock solutions of PEG-4SH and PEG-4VS were prepared in FBS free DMEM media at a concentration of 11 % (w/v). Stock solutions to make four 15 µl hydrogels were prepared as followed: the peptide solution was added (1.30 µl, 138.5 mM) to 42.08 µl of an 11% w/v PEG-4VS precursor solution and vortexed for one minute, then this solution was added to 7.01 µl of an 11% w/v PEG-4SH precursor solution and 9.61 µl of FBS free DMEM were added to the final solution to reach a solid content of 9 % (w/v).

Hydrogel mechanical properties

The time of gelation was measured by mixing the PEG-4SH with the PEG-4VS and transferring the solution on a rheometer plate (Anton Paar, Austria). The shear modulus was measured by oscillation at 10 rad.$^{s-1}$ with a 10% deformation and the intersection of the loss modulus with the storage modulus gave the time of gelation. The shear modulus of the hydrogel was measured by recording the loss and storage modulus from 1 to 100 rad/s. The storage modulus was reported for 60 rad/s. Mechanical properties of the hydrogels functionalised with CAP was measured by replacing the CAP with mercaptoethanol at the same concentration (24 mM).

Cell culture

Olfactory ensheathing cells (OECs) genetically modified to express a green fluorescent protein (GFP) were grown in T75 tissue culture flask in DMEM/F12 (supplemented with 10% FBS and 1% Pen-Strep) at 37 °C with 5% CO_2. Cells were passaged by removing the media, followed by three washing with dPBS (5 mL), trypsinised with TrypLE express enzyme (1 mL) and then incubated for 2 minutes. Detached cells were collected in 9 mL of media in a 15 mL Falcon tube and then centrifuged at 1000 rpm for 5 minutes. The supernatant was discarded, and the cell pellet was suspended in OECs medium (10 mL). Finally, the cells were re-seeded in T75 tissue culture flask. OECs were used until passage 11.

Hydrogel 3D cell cultures

PEG polymers were sterilized by freeze-drying and the dry powder PEG-4VS (15 mg) was diluted in 124.55 µl of serum-free media, the PEG-4SH (10 mg) was diluted in 82.71 µl of serum-free media to make an 11% w/v stock solution. The stock solution was prepared to make 4 gels with a volume of 15 µl each. The peptide solution was added (1.30 µl of 138.5 mM) to a PEG-4VS (42.08 µl of 11% solution) precursor solution. The solution was then vortexed for 1 minute. The cells were counted and suspended in DMEM without FBS with a final concentration of 1250 cells/µl. The cell suspension (9.61 µl) was added to the 7.01 µl of 11% solution PEG-4SH precursor solution. The solution of cells and PEG-4SH was then added to the solution containing PEG-4VS and peptide to form a hydrogel with a solid content of 9 % (w/v). Both solutions were mixed by vortexing for 10 seconds, and the solution was deposited in a microwell plate as a 15 µL droplet.

Peptide incorporation in the hydrogel

The content of peptide in the hydrogels was measured by X-ray Photoelectron Spectroscopy (XPS) with an AXIS Supra (XPS) surface analysis instrument using the ESCApe data acquisition and processing software from KRATOS analytical (Shimadzu Corporation of Kyoto, Japan). The spectra were analysed with CASA XPS software (Japan). For this analysis, two hydrogels were prepared, one hydrogel without any peptide and one with 3 mM of the CRGDSGK peptide. After gelation, the hydrogel was dried in a freeze dryer (Martin Christ, Germany) for 2 days. In each sample, percentage atomic concentrations were calculated and the amount of nitrogen was compared.

Peptide screening

The automated peptide screening in 3D hydrogels was performed on a QIAgility (Qiagen, Germany). The 3D hydrogels loaded with cells and different peptides were conducted in 384 glass-bottom well plates (capacity 125 µL/well). The liquid handling protocol was programmed in the QIAgility Setup Manager Software (Qiagen, Germany). We

made 15 µL hydrogels per well in a 384 well plate. The solutions were defined as viscous, and the mixing steps, pipette speed was set at 60 µl/sec. First, the 11% w/v PEG stock solution (4VS & 4SH) were prepared manually. Both polymer precursor solutions were placed in separate 1.5 mL tubes. Peptide stock solution of 138.5 mM concentration was further diluted to 24 mM and was placed in 200 µl strip tubes. Cells were passaged, counted and the resulting cell suspension (1500 cells/µL) was added to a 1.5 ml tube. Tips and empty microwell plates were placed in the robot and exposed to UV for 15 mins to sterilize the robot's workspace. The HEPA filter fan was switched on, the prepared solutions were placed on the robot's workspace and the experiment was run. First, the robot dispensed the crosslinker PEG-4SH (2 µL) into a 384 well plate. Then the master mix was made in a 96 well plate by mixing the peptide (3 µL), PEG-4VS (33 µL) and the cell suspension (3 µL). The master mix solution was mixed 3 times by oscillating pipetting. Then the master mix (13 µL) was added to the PEG-4SH solution in the 384 well plate and mix 3 times by oscillating pipetting. Each condition was prepared in triplicate. The mixture was allowed to gel for 20 mins and 100 µl of cell culture media was added on top. The media was replenished every day for 14 days.

Fluorescent microscopy

Fluorescent images were obtained on an inverted microscope Eclipse Tis, (Nikon, Japan) equipped with a suitable filter for GFP and confocal images were taken on a Nikon A1R confocal microscope (Nikon, Japan) using the software NIS-Elements (Nikon, Japan). The images were further processed by Image-J software.

Immunostaining

Immunostaining was conducted on cells cultured for 14 days in 3D peptide-functionalized hydrogels. The cells were fixed in the hydrogels with 4% paraformaldehyde solution and incubated for 35 minutes at room temperature. Sample permeabilization and blocking were done with a single solution. A solution of 4% w/v BSA in PBS (without divalent cations) was vortexed, filtered with the syringe fitted with a 0.22 µm Millex-GP Syringe filter (Sigma Aldrich, Australia) and 0.1% w/v Triton X was added and vortexed for 1 minute. The permeabilization/blocking solution was added to the samples and incubated for 12 hours at 4°C. This solution was then removed and the samples were washed three times with PBS. The antibody solution was prepared by diluting the primary antibody p75NTR (raised in rabbit) in 4% BSA solution diluted to 1:100. 200 µl of the primary antibody solution was added to the samples and allowed to incubate for 12hrs at 4°C. The samples were washed two times with PBS. The secondary antibody solution was made of Alexa Fluor™ 488 (ThermoFisher, USA) both raised in donkey against rabbit and rat respectively. The secondary antibody was solubilized in a 4% BSA solution diluted to 1:200. The secondary antibody added to the samples and incubated in the dark for 16hrs at 4°C. The samples were washed two times with PBS. The nuclei staining solution was made by diluting a DAPI 300 µM stock solution to 1:1000 in PBS. The diluted DAPI solution was placed over the samples for thirty minutes at room temp in the dark. The samples were washed two times with PBS and stored in the dark at 4°C until imaging.

Cell proliferation assay

The metabolic activity of cells was assessed with a Water Soluble Tetrazolium salt (WST-1) cell proliferation assay. First, 10µl of reagent was added to the samples with 100 µl DMEM media. The well plate with the samples and blanks was incubated at 37°C, 5% CO_2 for 4 hours. After incubation, the media was collected and transferred to a 96 well plate, the absorbance was measured on a xMark microplate absorbance spectrophotometer (Bio-rad, USA) at 450 nm wavelength and the results were corrected by subtracting the absorbance with a reference filter of 650 nm. The statistical analysis was performed to find the p-value by two-tailed T-test on Microsoft Excel software.

Conclusion

With an increase of the knowledge on cell-adhesion, short peptides are now available to help designing hydrogels that can direct cell organization and proliferation. However, testing CAPs for a specific cell type and a specific application is a tedious and complicated task that has led to the use of a limited number of CAP being used for tissue engineering purposes. This work proposes a strategy for going beyond RGD. We demonstrate that screening hydrogels functionalized with a library of CAPs can help to identify promising peptide sequences to direct the organization of OECs into structures relevant for the repair of spinal cord injuries. These results demonstrate the potential of screening of CAPs in 3D hydrogels and are stimulating to investigate non-conventional CAPs sequences further to prepare designer hydrogels for specific cell types and applications.

Acknowledgments

This work was supported by the DAAD PPP Australien 2020, Projekt-ID 57511846 and by the University of Freiburg Innovationsfonds 2019, Projekt 2100297201.

References

[1] Mann B K and West J L 2002 Cell adhesion peptides alter smooth muscle cell adhesion, proliferation, migration, and matrix protein synthesis on modified surfaces and in polymer scaffolds *J. Biomed. Mater. Res.* **60** 86–93

[2] Nakaoka R, Hirano Y, Mooney D J, Tsuchiya T and Matsuoka A 2013 Study on the potential of RGD- and PHSRN-modified alginates as artificial extracellular

matrices for engineering bone *J. Artif. Organs* **16** 284–93

[3] Malinen MM, Kanninen L K, Corlu A, Isoniemi H M, Lou Y R, Yliperttula M L and Urtti A O 2014 Differentiation of liver progenitor cell line to functional organotypic cultures in 3D nanofibrillar cellulose and hyaluronan-gelatin hydrogels *Biomaterials* **35** 5110–21

[4] Peela N, Sam F S, Christenson W, Truong D, Watson A W, Mouneimne G, Ros R and Nikkhah M 2016 A three dimensional micropatterned tumor model for breast cancer cell migration studies *Biomaterials* **81** 72–83

[5] Forget A, Christensen J, Lüdeke S, Kohler E, Tobias S, Matloubi M, Thomann R and Shastri V P 2013 Polysaccharide hydrogels with tunable stiffness and provasculogenic properties via α-helix to β-sheet switch in secondary structure *Proc. Natl. Acad. Sci.* **110** 12887–92

[6] Valarmathi M T, Davis J M, Yost M J, Goodwin R L and Potts J D 2009 A three-dimensional model of vasculogenesis *Biomaterials* **30** 1098–112

[7] Nakatsu M N, Sainson R C a., Aoto J N, Taylor K L, Aitkenhead M, Pérez-del-Pulgar S, Carpenter P M and Hughes C C W 2003 Angiogenic sprouting and capillary lumen formation modeled by human umbilical vein endothelial cells (HUVEC) in fibrin gels: the role of fibroblasts and Angiopoietin-1☆ *Microvasc. Res.* **66** 102–12

[8] Benton G, Arnaoutova I, George J, Kleinman H K and Koblinski J 2014 Matrigel: From discovery and ECM mimicry to assays and models for cancer research *Adv. Drug Deliv. Rev.* **79** 3–18

[9] Arya N, Forget A, Sarem M and Shastri V P 2019 RGDSP functionalized carboxylated agarose as extrudable carriers for chondrocyte delivery *Mater. Sci. Eng. C* **99** 103–11

[10] Forget A, Gianni-Barrera R, Uccelli A, Sarem M, Kohler E, Fogli B, Muraro M G, Bichet S, Aumann K, Banfi A and Shastri V P 2019 Mechanically Defined Microenvironment Promotes Stabilization of Microvasculature, Which Correlates with the Enrichment of a Novel Piezo-1 $^{+}$ Population of Circulating CD11b $^{+}$ /CD115 $^{+}$ Monocytes *Adv. Mater.* **1808050** 1808050

[11] Lozano R, Stevens L, Thompson B C, Gilmore K J, Gorkin R, Stewart E M, in het Panhuis M, Romero-Ortega M and Wallace G G 2015 3D printing of layered brain-like structures using peptide modified gellan gum substrates *Biomaterials* **67** 264–73

[12] Huettner N, Dargaville T R and Forget A 2018 Discovering Cell-Adhesion Peptides in Tissue Engineering: Beyond RGD *Trends Biotechnol.* **xx** 1–12

[13] Rape A D, Zibinsky M, Murthy N and Kumar S 2015 A synthetic hydrogel for the high-throughput study of cell-ECM interactions. *Nat. Commun.* **6** 8129

[14] Sharma S, Floren M, Ding Y, Stenmark K R, Tan W and Bryant S J 2017 A photoclickable peptide microarray platform for facile and rapid screening of 3-D tissue microenvironments *Biomaterials* **143** 17–28

[15] Seo J, Shin J Y, Leijten J, Jeon O, Camci-Unal G, Dikina A D, Brinegar K, Ghaemmaghami A M, Alsberg E and Khademhosseini A 2018 High-throughput approaches for screening and analysis of cell behaviors *Biomaterials* **153** 85–101

[16] Ramón-Cueto A and Avila J 1998 Olfactory ensheathing glia: properties and function *Brain Res. Bull.* **46** 175–87

[17] Féron F, Perry C, Cochrane J, Licina P, Nowitzke A, Urquhart S, Geraghty T and Mackay-Sim A 2005 Autologous olfactory ensheathing cell transplantation in human spinal cord injury *Brain* **128** 2951–60

[18] Tisay K T and Key B 1999 The extracellular matrix modulates olfactory neurite outgrowth on ensheathing cells *J. Neurosci.* **19** 9890–9

[19] Khankan R R, Wanner I B and Phelps P E 2015 Olfactory ensheathing cell–neurite alignment enhances neurite outgrowth in scar-like cultures *Exp. Neurol.* **269** 93–101

[20] Yang H, He B R and Hao D J 2014 Biological Roles of Olfactory Ensheathing Cells in Facilitating Neural Regeneration: A Systematic Review *Mol. Neurobiol.* **51** 168–79

[21] Boruch A V., Conners J J, Pipitone M, Deadwyler G, Storer P D, Devries G H and Jones K J 2001 Neurotrophic and migratory properties of an olfactory ensheathing cell line *Glia* **33** 225–9

[22] Wright A A, Todorovic M, Tello-Velasquez J, Rayfield A J, St John J A and Ekberg J A 2018 Enhancing the Therapeutic Potential of Olfactory Ensheathing Cells in Spinal Cord Repair Using Neurotrophins *Cell Transplant.* **27** 867–78

[23] Lutolf M P and Hubbell J a 2003 Synthesis and physicochemical characterization of end-linked poly(ethylene glycol)-co-peptide hydrogels formed by Michael-type addition. *Biomacromolecules* **4** 713–22

[24] Thiele J, Ma Y, Bruekers S M C, Ma S and Huck W T S 2014 25th anniversary article: Designer hydrogels for cell cultures: A materials selection guide *Adv. Mater.* **26** 125–48

[25] Zalipsky S 1995 Functionalized Poly(Ethylene Glycols) for Preparation of Biologically Relevant Conjugates *Bioconjug. Chem.* **6** 150–65

[26] Kim J, Kong Y P, Niedzielski S M, Singh R K, Putnam A J and Shikanov A 2016 Characterization of the crosslinking kinetics of multi-arm poly(ethylene glycol) hydrogels formed via Michael-type addition *Soft Matter* **12** 2076–85

[27] Wang S, Dalton P D and Dargaville T R 2018 Spatial Patterning of Hydrogels via 3D Covalent Transfer Stamping from a Fugitive Ink *Macromol. Rapid Commun.* **39** 3–7

[28] Wang H, Cheng F, Li M, Peng W and Qu J 2015 Reactivity and kinetics of vinyl sulfone-functionalized self-assembled monolayers for bioactive ligand immobilization *Langmuir* **31** 3413–21

[29] Engler A J, Sen S, Sweeney H L and Discher D E 2006 Matrix elasticity directs stem cell lineage specification. *Cell* **126** 677–89

[30] Budday S, Sommer G, Birkl C, Langkammer C, Haybaeck J, Kohnert J, Bauer M, Paulsen F, Steinmann P, Kuhl E and Holzapfel G A 2017 Mechanical characterization of human brain tissue *Acta Biomater.* **48** 319–40

[31] Urbanczyk C A, Palmeri M L and Bass C R 2015 Material characterization of in vivo and in vitro porcine brain using shear wave elasticity *Ultrasound Med. Biol.* **41** 713–23

[32] Johnson C L, Schwarb H, D.J. McGarry M, Anderson A T, Huesmann G R, Sutton B P and Cohen N J 2016 Viscoelasticity of subcortical gray matter structures *Hum. Brain Mapp.* **37** 4221–33

[33] Caliari S R and Burdick J A 2016 A practical guide to hydrogels for cell culture. *Nat. Methods* **13** 405–14

[34] Ekberg J A K, Amaya D, MacKay-Sim A and St. John J A 2012 The migration of olfactory ensheathing cells during development and regeneration *NeuroSignals* **20** 147–58

[35] Haggerty A E, Marlow M M and Oudega M 2017

Extracellular matrix components as therapeutics for spinal cord injury *Neurosci. Lett.* **652** 50–5

[36] Icer M A and Gezmen-Karadag M 2018 The multiple functions and mechanisms of osteopontin *Clin. Biochem.* **59** 17–24

[37] Zhao H, Chen Q, Alam A, Cui J, Suen K C, Soo A P, Eguchi S, Gu J and Ma D 2018 The role of osteopontin in the progression of solid organ tumour *Cell Death Dis.* **9** 356

[38] Sharma A 1999 Crystal structure of a heparin-and integrin-binding segment of human fibronectin *EMBO J.* **18** 1468–79

[39] Dee K C, Andersen T T and Bizios R 1998 Design and function of novel osteoblast-adhesive peptides for chemical modification of biomaterials *J. Biomed. Mater. Res.* **40** 371–7

[40] Lee M H, Adams C S, Boettiger D, DeGrado W F, Shapiro I M, Composto R J and Ducheyne P 2007 Adhesion of MC3T3-E1 cells to RGD peptides of different flanking residues: Detachment strength and correlation with long-term cellular function *J. Biomed. Mater. Res. Part A* **81A** 150–60

[41] Sandvig I, Karstensen K, Rokstad A M, Aachmann F L, Formo K, Sandvig A, Skjåk-Braek G and Strand B L 2015 RGD-peptide modified alginate by a chemoenzymatic strategy for tissue engineering applications *J. Biomed. Mater. Res. Part A* **103** 896–906

[42] Cui F Z, Tian W M, Hou S P, Xu Q Y and Lee I S 2006 Hyaluronic acid hydrogel immobilized with RGD peptides for brain tissue engineering *Journal of Materials Science: Materials in Medicine*

[43] Mould A P and Humphries M J 1991 Identification of a novel recognition sequence for the integrin alpha 4 beta 1 in the COOH-terminal heparin-binding domain of fibronectin. *EMBO J.* **10** 4089–95

[44] Hozumi K, Nakamura K, Hori H, Miyagi M, Nagao R and Takasaki K 2016 Mixed Fibronectin-Derived Peptides Conjugated to a Chitosan Matrix Effectively Promotes Biological Activities through Integrins , a 4 b 1 , a 5 b 1 , a v b 3 , and Syndecan **5** 356–66

[45] Tomaselli K J, Hall D E, Flier L A, Gehlsen K R, Turner D C, Carbonetto S and Reichardt L F 1990 A neuronal cell line (PC12) expresses two β 1 -class integrins-α 1 β 1 , and α 3 β 1 -that recognize different neurite outgrowth-promoting domains in laminin *Neuron* **5** 651–62

[46] Kibbey M C, Jucker M, Weeks B S, Neve R L, Van Nostrand W E and Kleinman H K 1993 beta-Amyloid precursor protein binds to the neurite-promoting IKVAV site of laminin. *Proc. Natl. Acad. Sci.* **90** 10150–3

[47] Ponce M L, Nomizu M and Kleinman H K 2002 An angiogenic laminin site and its antagonist bind through the αvβ3 and α5β1 integrins *FASEB J.* **15** 1389–97

[48] Nakahara H, Nomizu M, Akiyama S K, Yamada Y, Yeh Y and Chen W-T 2002 A Mechanism for Regulation of Melanoma Invasion *J. Biol. Chem.* **271** 27221–4

[49] Maeda T, Titani K and Sekiguchi K 1994 Cell-adhesive activity and receptor-binding specificity of the laminin-derived YIGSR sequence grafted onto Staphylococcal protein a *J. Biochem.* **115** 182–9

[50] Smith Callahan L A, Xie S, Barker I A, Zheng J, Reneker D H, Dove A P and Becker M L 2013 Directed differentiation and neurite extension of mouse embryonic stem cell on aligned poly(lactide) nanofibers functionalized with YIGSR peptide *Biomaterials* **34** 9089–95

[51] Bayless K J and Davis G E 2001 Identification of Dual α4β1 Integrin Binding Sites within a 38 Amino Acid Domain in the N-terminal Thrombin Fragment of Human Osteopontin *J. Biol. Chem.* **276** 13483–9

[52] Wojtowicz A M, Shekaran A, Oest M E, Dupont K M, Templeman K L, Hutmacher D W, Guldberg R E and García A J 2010 Coating of biomaterial scaffolds with the collagen-mimetic peptide GFOGER for bone defect repair *Biomaterials* **31** 2574–82

[53] Mehta M, Madl C M, Lee S, Duda G N and Mooney D J 2015 The collagen i mimetic peptide DGEA enhances an osteogenic phenotype in mesenchymal stem cells when presented from cell-encapsulating hydrogels *J. Biomed. Mater. Res. - Part A* **103** 3516–25

[54] Floquet N, Pasco S, Ramont L, Derreumaux P, Laronze J Y, Nuzillard J M, Maquart F X, Alix A J P and Monboisse J C 2004 The Antitumor Properties of the α3(IV)-(185-203) Peptide from the NC1 Domain of Type IV Collagen (Tumstatin) Are Conformation-dependent *J. Biol. Chem.* **279** 2091–100

[55] García-Arévalo C, Pierna M, Girotti A, Arias F J and Rodríguez-Cabello J C 2012 A comparative study of cell behavior on different energetic and bioactive polymeric surfaces made from elastin-like recombinamers *Soft Matter* **8** 3239–49

[56] Li Z, Calzada M J, Sipes J M, Cashel J A, Krutzsch H C, Annis D S, Mosher D F and Roberts D D 2002 Interactions of thrombospondins with α4β1 integrin and CD47 differentially modulate T cell behavior *J. Cell Biol.* **157** 509–19

[57] Calzada M J, Sipes J M, Krutzsch H C, Yurchenco P D, Annis D S, Mosher D F and Roberts D D 2003 Recognition of the N-terminal Modules of Thrombospondin-1 and Thrombospondin-2 by α 6 β 1 Integrin *J. Biol. Chem.* **278** 40679–87

[58] Velasquez J T, Watts M E, Todorovic M, Nazareth L, Pastrana E, Diaz-Nido J, Lim F, Ekberg J A K, Quinn R J and St John J A 2014 Low-dose curcumin stimulates proliferation, migration and phagocytic activity of olfactory ensheathing cells *PLoS One* **9**